ELSEVIER

Thermochimica Acta 261 (1995) 209–220

thermochimica acta

The role of cobalt in the oxidation mechanism modification of the Mo^{3+} ions of molybdenum-substituted magnetites

E. Kester [a], B. Gillot *,[a], L. Bouet [b], P. Tailhades [b], A. Rousset [b]

[a] *Laboratoire de Recherches sur la Réactivité des Solides, URA 23, Faculté des Sciences Mirande, B.P. 138, 21004 Dijon Cedex, France*

[b] *Laboratoire de Chimie des Matériaux Inorganiques, URA 1311, Université Paul Sabatier, 118 route de Narbonne, 31062 Toulouse Cedex, France*

Received 30 September 1994; accepted 26 February 1995

Abstract

A kinetic study of the oxidation of Mo^{3+} ions has been performed on two submicrometer Mo and Mo–Co ferrites of spinel structure with a nearly identical molybdenum content. We show that for the Co-free sample, oxidation proceeds by cationic diffusion in a cation-deficient spinel with a variable chemical diffusion coefficient. For the Co sample, which showed a pronounced stability towards oxygen, the oxidation process was divided into three steps. In step I, oxidation declines with time in an initial period (degree of oxidation $\alpha < 0.1$). In step II ($0.1 < \alpha < 0.25$), oxidation is accelerated and in step III ($\alpha > 0.25$) oxidation is best described by the diffusion-controlled Jander equation. Comparing the vibrational spectra of these two spinels after total oxidation for various thermal treatments, we conclude that the coordination around Mo^{6+} ions changes from tetrahedral to octahedral with Co substitution and that the location of cobalt and molybdenum ions in octahedral sites changes with the annealing process.

Keywords: Cobalt role; Mo^{6+} coordination; Molybdenum-substituted magnetite; Oxidation mechanism; Vibrational spectrum

1. Introduction

The role of cobalt in the control of the magnetic properties of ferrites with spinel structure is well documented [1–3]. Recently, the variation of the coercivity of

* Corresponding author.

SSDI 0040-6031(95)02324-0

submicron $Mn_xCo_yFe_{3-x-y}O_4$ and $Mo_xCo_xFe_{3-x-y}O_4$ ferrite particles during their oxidation in cation-deficient spinels has been studied [4–7]. The originality of these compounds, in comparison with other defect ferrites, is that the vacancies result not only from the oxidation of Fe^{2+} ions but also from the oxidation of Mn^{2+} and Mn^{3+} ions or Mo^{3+} and Mo^{4+} ions. These vacancies enhance or hinder the movement of cobalt ions between equivalent cation sites and cause the directional order phenomenon that has the property of greatly increasing the coercive field for each oxidized cation. This means that the oxidation state and distribution of the cations on the spinel lattice largely determine the original properties of these non-stoichiometric spinels, such as their magnetic and electrical properties [8].

In this paper we compare the results of a study of the oxidation mechanism of two series of samples synthesized at low temperature. The first is molybdenum-substituted magnetite, $Fe_{3-x}Mo_xO_4$ with $x = 0.17$, and the second Co–molybdenum-substituted magnetite $Mo_xCo_yFe_{3-x-y}O_4$ with $x = 0.165$ and $y = 0.85$; it has been demonstrated that in both cases iron and molybdenum ions can be oxidized below 500°C giving cation-deficient spinels [7]. In addition, we report here the kinetic results of Mo^{3+} ion oxidation in non-isothermal and isothermal conditions, and present the first results of a Fourier transform infrared (FTIR) analysis providing information on Mo^{6+} ion coordination in the spinel lattice and the changes induced upon thermal treatment, in order to have a better understanding of the magnetic properties of the materials.

2. Samples and analytical methods

The Mo- and Co–Mo-substituted ferrites were synthesized as follows. The Mo series was prepared by precipitation of Fe^{2+}, Fe^{3+} and Mo^{5+} chloride in alkaline medium (NH_4OH), followed by a heat treatment as reported in Ref. [9]. A second treatment of the precipitated mixed oxides (α-Fe_2O_3 and $Fe_2(MoO_4)_3$) under an N_2–H_2–H_2O mixture at around 500°C yielded the spinel phase. The Co–Mo-substituted ferrite was obtained from precipitation of the chloride by oxalic acid in an alcoholic medium [5] followed by an annealing treatment and a reduction. The spinel phases were fine grained with a mean crystallite size close to 50 nm.

Using thermogravimetry under very strict and well-defined experimental conditions, we have shown [10] that these finely divided powders can be oxidized at specific temperatures characteristic of each oxidizable cation at either octahedral B or tetrahedral A sites. For example, it has been demonstrated [11] that in the case of the molybdenum-substituted magnetites, Fe_B^{2+}, Mo_B^{3+}, Mo_B^{4+}, and Fe_A^{2+} are successively oxidized into Fe^{3+} and Mo^{6+} ions leading to four distinct oxidation reactions

$$3Fe_B^{2+} \rightarrow 2Fe_B^{3+} + \square \quad \text{at } 200°C \tag{1}$$

$$3Mo_B^{3+} \rightarrow Mo^{6+} + \square \quad \text{at } 280°C \tag{2}$$

$$3Mo_B^{4+} \rightarrow 2Mo^{6+} + \square \quad \text{at } 340°C \tag{3}$$

$$3Fe_A^{2+} \rightarrow 2Fe_A^{3+} + \square \quad \text{at } 380°C \tag{4}$$

Thereby, the determination of the cationic distribution can be performed from a quantitative analysis by DTG [11] where the desummation of the DTG curves permits four separate oxidation peaks to be distinguished, the area of each peak being indicative of the quantities of each oxidizable cation within the spinel. For $Fe_{2.83}Mo_{0.17}O_4$ spinel, the cationic distribution may be described by a structural formula as [11]

$$(Fe^{2+}_{0.03}Fe^{3+}_{0.97})_A(Mo^{3+}_{0.147}Mo^{4+}_{0.018}Fe^{2+}_{0.99}Fe^{3+}_{0.85})_BO^{2-}_4 \quad (5)$$

For $Fe_{1.985}Mo_{0.165}Co_{0.85}O_4$ spinel when the Fe^{2+} ions are for the most part replaced by Co^{2+} ions at B sites, this cationic formula becomes

$$(Fe^{2+}_{0.1}Fe^{3+}_{0.9})_A(Mo^{3+}_{0.14}Mo^{4+}_{0.025}Fe^{2+}_{0.075}Fe^{3+}_{0.91}Co^{2+}_{0.85})_BO^{2-}_4 \quad (6)$$

The oxidations were performed in a static atmosphere of pure O_2 ($P_{O_2} = 5 \times 10^3$ Pa) under isothermal conditions or with the temperature increasing at a linear rate (2°C min^{-1}) in a Setaram MTB 10-8 microbalance starting with 10 mg of powder. The degree of oxidation of the samples at various levels of reaction was calculated from the gravimetric data.

The IR spectra were recorded with a Perkin-Elmer 1725X FTIR spectrometer over the range 4000–400 cm^{-1} and with a Perkin-Elmer 1700 FTIR spectrometer over the range 500–50 cm^{-1}. About 1 mg of sample was mixedwith 200 mg of spectroscopically pure dry CsI and pressed into disks before recording the spectra.

3. Results and discussion

3.1. Non-isothermal oxidation

A close examination of the influence of cobalt substitution reveals that the area of each peak is profoundly modified by the substitution of iron by cobalt (Fig. 1, curves a and b). In particular, the drastic decrease in the area of the first peak (curve b) arises from the substitution of Fe^{2+} ions by Co^{2+} at the B sites. Considering the strong preference of Co^{2+} ions for B sites in $CoFe_2O_4$, it is inferred that the concentration of Fe^{2+} ions would be decreased upon substitution. Fig. 1 also shows that the presence of cobalt modifies the peak shape of Mo^{3+} ions (curve b) under oxidizing conditions, thus suggesting a change in the oxidation mechanism. In addition, the peak areas for oxidation of Mo^{4+} ions at the B sites and Fe^{2+} ions at the A sites are substantially increased, revealing that the preparation method, i.e. decomposition in a controlled atmosphere of hydroxide or oxalic precursors, must modify the cationic distribution. For instance, the fast electron transfer due to the mixed valence of both the Fe and Mo on the A and the B sites is related to cation distribution when the main equilibria in the ferrites are

$$Fe^{2+}_A Fe^{3+}_B Mo^{3+}_B \rightleftharpoons Fe^{3+}_A Fe^{2+}_B Mo^{3+}_B \rightleftharpoons Fe^{2+}_A Fe^{2+}_B Mo^{4+}_B \quad (7)$$

Another difference resides in the FTIR spectra which indicate a change in the coordination of Mo^{6+} ions from tetrahedral to octahedral with cobalt substitution.

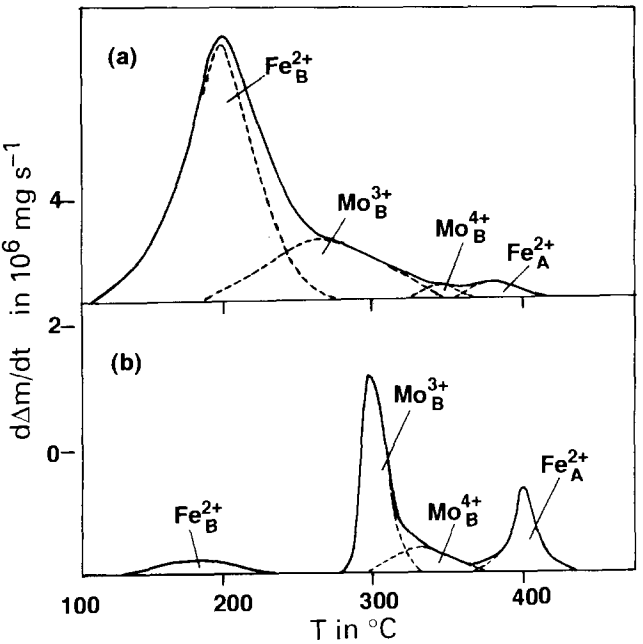

Fig. 1. DTG curves of samples heated in pure O_2 ($P_{O_2} = 2 \times 10^3$ Pa) at a linear rate of 2°C min^{-1}: (a) Mo-substituted magnetite; (b) Mo–Co-substituted magnetite.

For the Co sample, three high-frequency absorption bands at 788, 861 and 930 cm^{-1} are detected after oxidation at 400°C (Fig. 2, curves b and c), indicating the presence of a distorted octahedral coordination of Mo similar to that found in molybdates of Co(II) or Fe(II) [12,13]. As previously shown [14], this octahedral coordination symmetry around Mo^{6+} ions remains because of the presence of a divalent cation at the B sites, suggesting a strong interaction of molybdenum with the divalent cation leading to the formation of Mo–Co, Mo–Fe or Mo–Co–Fe ion associations in the surface layer.

For the Co-free sample after oxidation, the IR spectrum exhibits (Fig. 2, curve f) only two high-frequency absorption bands at 840 and 960 cm^{-1} which may be associated with the presence of Mo^{6+} ions at the A sites [15]. They are attributed to isolated MoO_4 tetrahedra and are similar to those found in $Na_2MoO_4 \cdot 2H_2O$ [16] or $Fe_2(MoO_4)_3$ in which the molybdenum is tetrahedrally coordinated by oxygens. Thus the original octahedral coordination of Mo^{6+} ions in Co–molybdenum ferrites is transformed into a tetrahedral coordination in Co-free ferrite and the oxidizability of Mo^{3+} ions is strongly decreased in the presence of Co^{2+} ions.

3.2. *Isothermal oxidation*

The possibility for every cation to be oxidized independently by selective oxidation [14] enables us to study the oxidation kinetics of the various oxidizable ions, particularly that of Mo^{3+} ions because in presence of Co^{2+} ions the oxidation

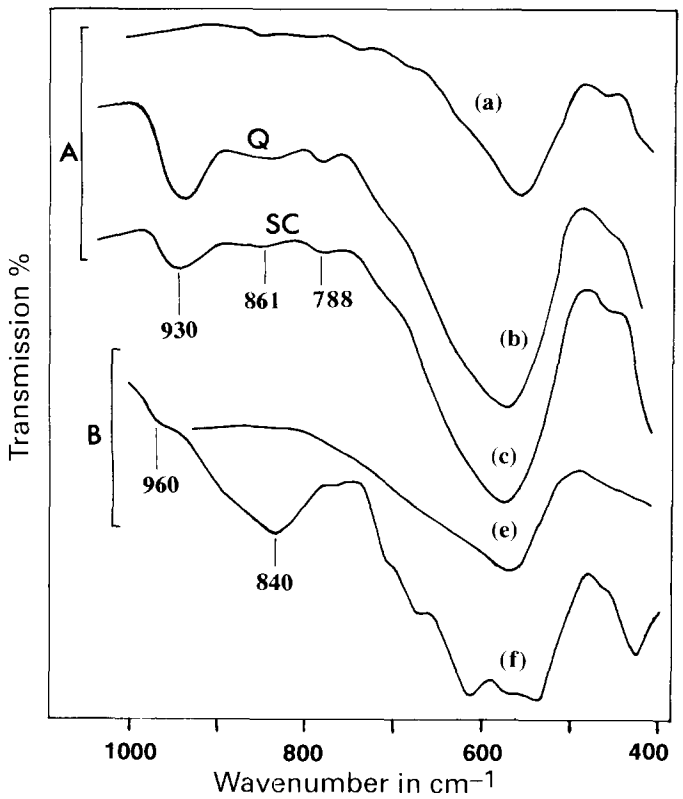

Fig. 2. Determination of the Mo^{6+} coordination from the IR spectra in the 1000–400 cm^{-1} region. A. Mo–Co-substituted magnetite: (a) before oxidation; after oxidation at 400°C, (b) Q sample, (c) SC sample. B. Mo-substituted magnetite: (e) before oxidation, (f) after oxidation at 400°C.

mechanism was apparently modified. After total oxidation of the Fe^{2+} ions at the B sites (at 155°C for 24 h), the oxidation of the octahedral Mo^{3+} ions can be studied at different isothermal temperatures. However for both samples with or without Co, the oxidation of Mo^{3+} ions is carried out from a cation-deficient spinel that contains a different amount of vacancies. Whereas for Co-free spinel the amount of vacancies resulting from Fe^{2+} ion oxidation approaches that found in γ-Fe_2O_3, leading to the cationic distribution

$$(Fe^{2+}_{0.026}Fe^{3+}_{0.974})_A(Mo^{3+}_{0.129}Mo^{4+}_{0.016}Fe^{3+}_{1.523}\square_{0.332})_B O^{2-}_4 \quad (8)$$

substitution of the Fe^{2+} ions by Co^{2+} ions considerably diminishes the amount of vacancies, because for this cation-deficient spinel the cationic distribution can be formulated as

$$(Fe^{2+}_{0.099}Fe^{3+}_{0.901})_A(Mo^{3+}_{0.139}Mo^{4+}_{0.025}Fe^{3+}_{0.977}Co^{2+}_{0.83}\square_{0.03})_B O^{2-}_4 \quad (9)$$

where $\square$ denotes vacancies.

The fraction of reaction completed (α_{Mo}) as a function of time for each system and isotherm run is shown in Figs. 3 and 4. This fraction is referred to the oxidation of Mo^{3+} ions only in the temperature range 232–265°C for the Co-free sample and 288–332°C for the Co sample. Inspection of Fig. 3 shows that the reaction for the Co-free material is continuously decelerated in all cases, following an approximate parabolic rate law. This is the behavior expected for a diffusion-controlled process. However, a total analogy with the kinetic curves found for Fe^{2+} ion oxidation in submicrometer magnetites, considering a diffusion mechanism with a constant chemical diffusion coefficient $\tilde{D}$, is not observed [17]. This is assumed to be due to the decrease of $\tilde{D}$ with increasing vacancies content δ (Fig. 5). Such a decrease has already been explained by considering that very important stresses are generated in the grain during oxidation when the outside of the grain is more oxidized than the interior [18,19]. In these conditions, δ and consequently $\tilde{D}$ depend on the reaction time only and the data corresponding to each isothermal run were analyzed by the equation

$$\alpha_{Mo} = 1 - 6/\pi^2 \sum_{n=1}^{\infty} \frac{1}{n^2} \exp\left(-n^2 \frac{\pi^2}{a^2} \int_0^t \tilde{D}(t)\mathrm{d}t \right) \tag{10}$$

where a is the mean grain radius. From the variation of $\ln \tilde{D}$ versus $1/T$ for various α_{Mo} values, an activation energy of 156 kJmol^{-1} was obtained. For this spinel and after oxidation of Mo^{3+} ions, the cationic distribution can be written

$$(Fe^{2+}_{0.025}Fe^{3+}_{0.853}Mo^{6+}_{0.122})_A(Mo^{4+}_{0.015}Fe^{3+}_{1.527}\square_{0.458})_B O_4^{2-} \tag{11}$$

Isothermal runs for Co–Mo-substituted ferrite are represented in Fig. 4. The shape of these curves differs significantly from those of Co-free ferrite. The oxidation process

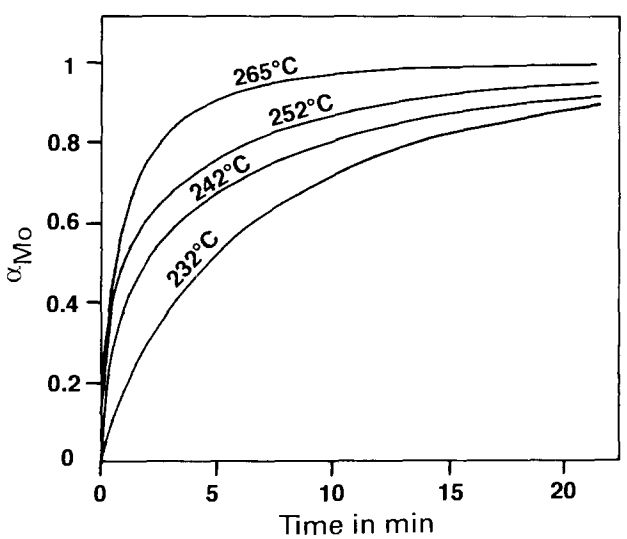

Fig. 3. Kinetic curves $\alpha Mo = f(t)$ for oxidation of octahedral Mo^{3+} ions in an Mo-substituted magnetite.

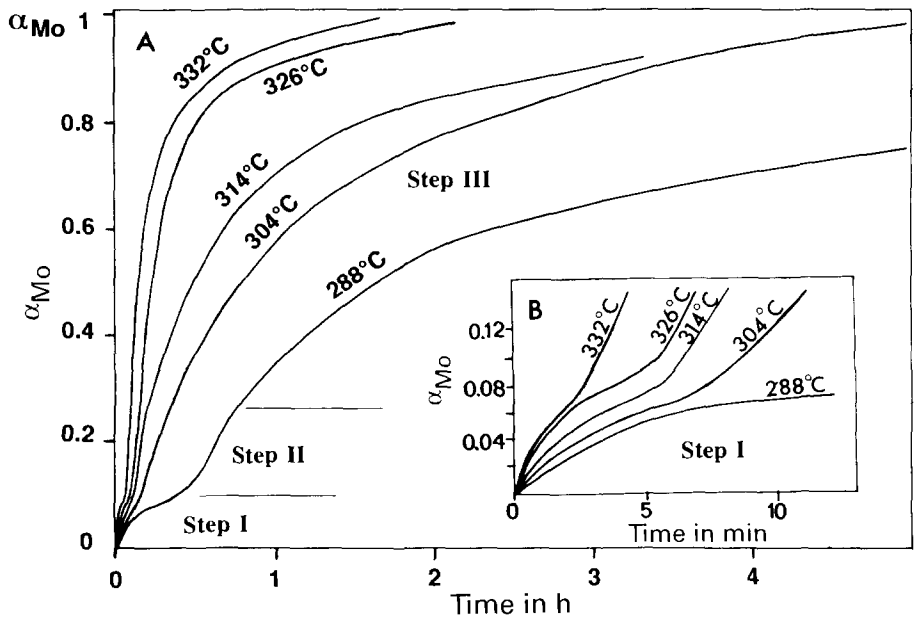

Fig. 4. Kinetic curves $\alpha Mo = f(t)$ for oxidation of octahedral Mo^{3+} ions in: A, Co–Mo-substituted magnetite; B, detail of A.

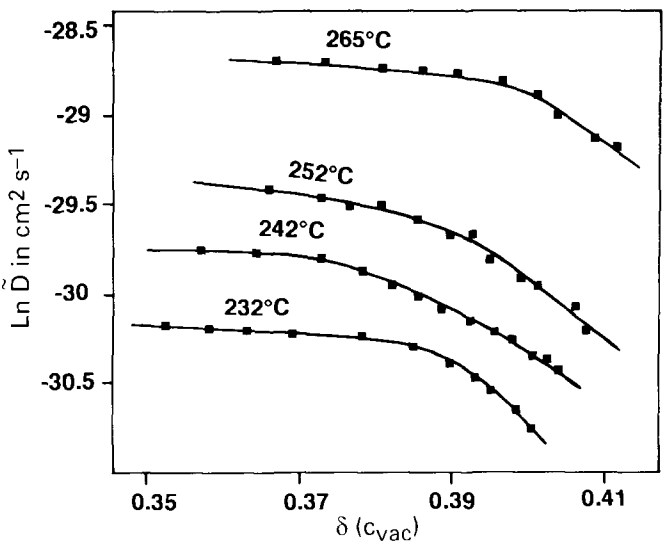

Fig. 5. Vacancy content dependence of the chemical diffusion coefficient for varous oxidation temperatures of Mo-substituted magnetite.

seems to be divided into three steps. A separate initial period (step I, $0 < \alpha < 0.10$) is observed and oxidation slowed down progressively with time over the whole temperature range of 288–332°C. The oxidation in this step failed to be represented by any diffusion law because of inaccuracies resulting from the narrow range of the conversion rate. However, the parabolic character of the kinetic curves would in such cases be due to oxidation of the Mo^{3+} ions probably present in a superficial layer of mixed molybdate formed during the preparation procedure. After step I, it was found that oxidation up to about $\alpha = 0.25$ presents an accelerated region. In this region, the kinetics of the reaction follows rather closely the law deduced by Prout and Tompkins [20]

$$\ln \alpha/1 - \alpha = kt + C \tag{12}$$

It must be recalled that an autocatalytic process can also be represented by Eq. (12) [21]. From the temperature dependence of k_1, an apparent activation energy of 150 kJ mol^{-1} was obtained. During this step, compact composite molybdate is probably formed in the outer layer of the particle in order to stabilize the octahedral coordination of Mo^{6+} ions always present on the particle surface. This stabilization results in the association of divalent cations, M^{2+}–Mo^{6+}($M^{2+} = Co^{2+}, Fe^{2+}$), with possible formation of $M^2 + Mo^{6+}O_4{}^{2-}$ complexes having the molybdate structure; this is a transformation product for temperatures above 500°C. This outer layer inhibits the diffusion of Mo^{3+} ions in the vicinity of the particle–gas interface. In the third step of the reaction ($0.30 < \alpha < 0.90$), when only a small amount of Mo^{3+} ions has been oxidized, further oxidation of spinel is best described by the diffusion-controlled Jander equation [22]

$$[1 - (1 - \alpha)^{1/3}]^2 = k_2 t \tag{13}$$

which assumes that the diffusion coefficient of the mobile species is independent of time. Plots of the left side of Eq. (13) versus time were found to fit straight lines as illustrated in Fig. 6. In this step, the activation energy of 186 kJ mol^{-1} derived from the slope of the corresponding straight lines is higher than that found for the oxidation of Co-free sample where it is shown that the diffusion also limits the oxidation of the spinel. Thus, it is suggested that the incorporation of Co affects the reaction rate and that the octahedral preference of Co^{2+} and Mo^{6+} ions makes migration of cations and vacancies through the spinel more difficult, leading to lower reactivity. After oxidation of the Mo^{3+} ions and assuming that Mo^{6+} ions occupy octahedral sites, the cationic distribution gives

$$(Fe^{2+}_{0.094}Fe^{3+}_{0.906})_A(Mo^{4+}_{0.024}Mo^{6+}_{0.132}Fe^{3+}_{0.872}Co^{2+}_{0.789}\square_{0.183})_B O^{2-}_4 \tag{14}$$

It should be emphasized that in this case the vacancy content δ is only caused by oxidation of Mo^{3+} ions yielding a considerably lower formal vacancy content than is obtained in the Mo-substituted magnetite oxidation (Eq. (11)). This explains, in part, why the chemical diffusion coefficient, which depends on δ from a significant amount of vacancies ($\delta > 0.20$), has been found to be effectively constant due to the fact that before oxidation of Mo^{3+} ions the vacancy content remains near zero and so the occurrence of stresses would be very small. As a matter of fact, such stresses are only caused by the

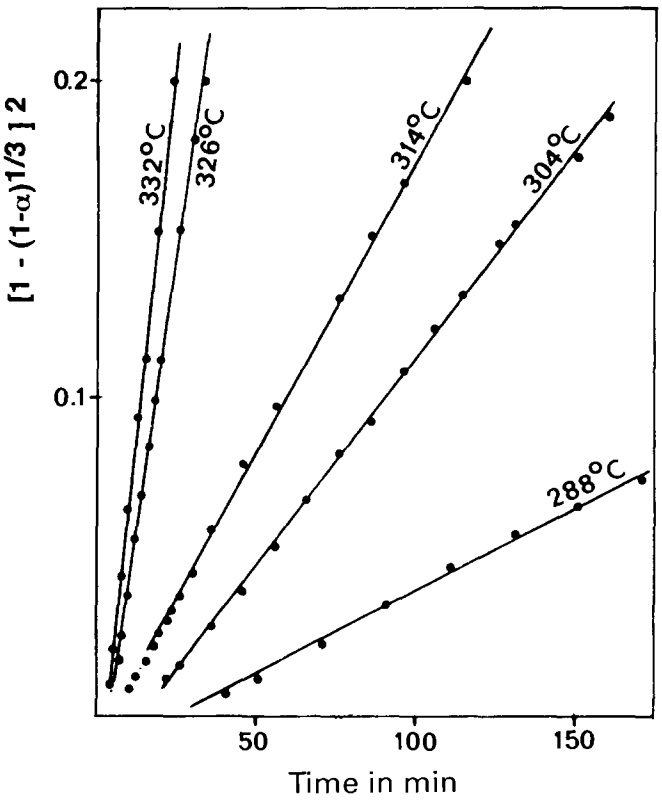

Fig. 6. Jander plots for isothermal oxidation kinetics of Mo–Co-substituted magnetite.

concentration gradient of the different species inside the grain, i.e. when the grain is more oxidized on its surface than in the bulk [23]. Consequently, for Co-substituted ferrites where the vacancy content remains low before oxidation of Mo^{3+} ions (the existence of stresses being only slightly likely) one would not observe a decrease in the chemical diffusion coefficient.

In this connection, it is interesting to compare the FTIR spectra of totally oxidized samples treated under different thermal conditions, i.e. slowly cooled (SC) or quenched (Q) samples, because it has previously been suggested that the increase in coercivity for slowly cooled defect ferrites is linked to the creation of a directional order [4]. Fig. 7 shows spectra of Co–Mo ferrite oxidized at 400°C for 4 h, and having undergone these two treatments (curves b and c). A marked difference appears in the slowly cooled sample (curve c): a large number of well-resolved absorption bands can be registered in the 500–100 cm^{-1} region, predicting a reorganization of cobalt ions. At this point, it should be mentioned that for the totally oxidized Co-free sample (Fig. 2, curve f and Fig. 7, curve f), a large number of absorption bands were also observed arising from the lower symmetry resulting from ordered cations and vacancies on B sites [24]. However,

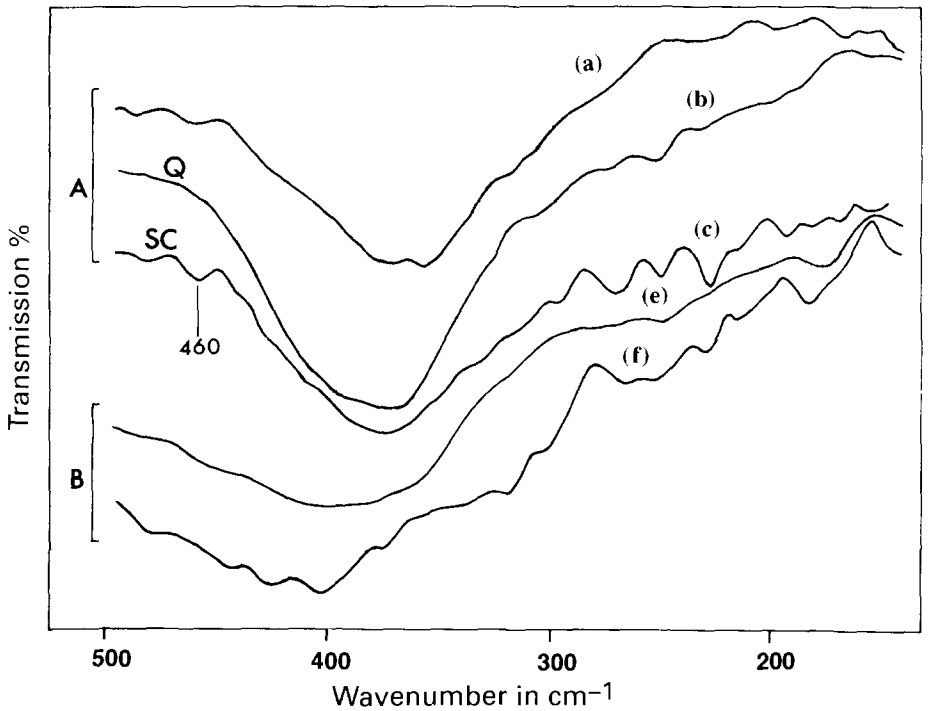

Fig. 7. IR spectra of oxidized samples at 400°C in the 500–150 cm^{-1} region. A. Mo–Co-substituted magnetite: (a) before oxidation, (b) for Q sample, (c) for SC sample. B. Mo-substituted magnetite: (e) before oxidation, (f) after oxidation.

the number and the frequencies of the observed bands are different from those obtained here for the Co sample. We believe that this reorganization leads to the appearance of additional lines which may be due to the lowering of the unit cell symmetry as a result of the distortion of the octahedron from cubic symmetry by Co^{2+} [1]. Moreover, as can be seen, the spectrum reveals an absorption band at around 460 cm^{-1} which was also observed in the initial sample (curve a) but that becomes a shoulder for cobalt ferrite $CoFe_2O_4$ [25]. In contrast to the quenched samples (curve b) which show a statistical distribution of cations at room temperature, the absorption band at 460 cm^{-1} is not observed, while the intensity of the strong band at 930 cm^{-1} (Fig. 2, curve c) attributed to Mo^{6+} ions at B sites increases compared to that of slowly cooled samples (Fig. 2, curve b).

After oxidation at 400°C when the Fe_B^{2+}, Mo_B^{3+}, Mo_B^{4+}, Fe_A^{2+} ions are oxidized, defect Co–Mo spinels may be described by the structural formula

$$(Fe^{3+})_A(Mo^{6+}_{0.153}Fe^{3+}_{0.839}Co^{2+}_{0.774}\square_{0.234})_B O_4^{2-} \quad (15)$$

The formation of mixed molybdate $Fe_{1-x}Co_xMoO_4$ of variable composition in the outer layer of the particle may explain the different concentration of Co in the particle, governed by the conditions of thermal treatment. This may be caused by the formation of $FeMoO_4$ (low value of x) in the outer layer of the particle instead of $CoMoO_4$ (large value of x) with increasing cooling rate.

4. Conclusion

The present study established that the substitution of cobalt in submicrometer $Fe_{2.83}Mo_{0.17}O_4$ spinel changes the oxidation mechanism related to the formation of cation-deficient spinel, as revealed by the non-isothermal oxidation and kinetic curves. The oxidation kinetics for a Co-free sample conforms to a diffusion-controlled process in the degree transformation region with a variable chemical diffusion coefficient, because the occurring stresses induced by the gradient of the different mobile species inside the grain result in a large number of vacancies. For the Co sample, the oxidation proceeds at a higher temperature. It was accelerated at 10–25% oxidation, not with a diffusion-controlled reaction, however, because a compact oxidized layer of molybdate was formed on the surface. The diffusion-controlled reaction operated only in the range of 30–90% oxidation where it is assumed that the diffusion of the remaining Mo^{3+} ions through the mixed molybdate layer limits the oxidation of the spinel and that the chemical diffusion coefficient in almost stress-free spinel is concentration-independent.

In this respect, we have also demonstrated a modification in the FTIR spectra appearing for totally oxidized Co–Mo-substituted magnetities as a function of cooling rate, which depends on the kinetics of cationic distribution and enhances or hinders the movement of cobalt ions in the spinel lattice. In particular, the reorganization of cobalt and molybdenum ions in octahedral sites for slowly cooled samples leads to the appearance of additional absorption bands in the IR spectra as a result of the lowering of the unit cell symmetry.

References

[1] J.C. Slonczewski, Phys. Rev., 110 (1958) 1341.
[2] L.R. Bickford, Jr., J.M. Brownlow and R.F. Penoyer, J. Appl. Phys., 29 (1958) 441.
[3] P. Mollard, A. Collomb, J. Devenyi and A. Rousset, J. Paris, IEEE Trans. Magn., MAG-11 (1975) 894.
[4] P. Mollard, P. Tailhades and A. Rousset, IEEE Trans. Magn., MAG-26 (1990) 241.
[5] P. Tailhades, P. Mollard, A. Rousset and M. Gougeon, IEEE Trans. Magn., MAG 26 (1990) 1822.
[6] P. Tailhades, Ch. Sarda, P. Mollard and A. Rousset, J. Magn. Magn. Mater, 104–107 (1992) 969.
[7] P. Tailhades, L. Bouet, B. Gillot, P. Mollard and A. Rousset, Proceedings of the 6th International Conference on Ferrites, Tokyo, 1992, p. 624.
[8] B. Gillot and A. Rousset, Heterogeneous Chem. Rev., 1 (1994) 69.
[9] L. Bouet, P. Tailhades, A. Rousset and B. Gillot, C.R. Acad. Sci., Paris, 312 Série II (1991) 1507.
[10] B. Gillot, J. Solid State Chem., 113 (1994) 163.
[11] B. Domenichini, B. Gillot, P. Tailhades, L. Bouet and A. Rousset, Solid State Ionics, 58 (1992) 61.
[12] P.P. Cord, P. Courtine, P. Pannetier and J. Guillemet, Spectrochim. Acta, A 28 (1972) 1601.

[13] F. Trifido, G. Gaputo and P. Villa, J. Less Common Met., 36 (1974) 305.
[14] B. Gillot, B. Domenichini, L. Bouet, P. Tailhades and A. Rousset, Solid State Ionics, 63–65 (1993) 620.
[15] B. Domenichini, B. Gillot, L. Bouet, P. Tailhades and A. Rousset, J. Solid State Chem., 103 (1993) 16.
[16] G.M. Clark and W.P. Doyle, Spectrochim. Acta, 21 (1965) 1333.
[17] B. Gillot, Ann. Chim. Fr., 3 (1978) 209.
[18] B. Domenichini and B. Gillot, Solid State Ionics, 57 (1992) 11.
[19] M. Nohair, P. Perriat, B. Domenichini and B. Gillot, Thermochim. Acta, 244 (1994) 223.
[20] E.G. Prout and F.C. Tompkins, Trans. Faraday Soc., 40 (1994) 488.
[21] W.D. Bond, J. Phys. Chem., 66 (1962) 1573.
[22] W. Jander, Z. Anorg. Allg. Chem., 163 (1927) 1.
[23] P. Perriat, B. Domenichini and B. Gillot, J. Phys. Chem. Solids, to be published.
[24] B. Gillot, Vibrational Spectroscopy, 6 (1994) 127.
[25] B. Gillot, J. Jemmali and A. Rousset, J. Solid State Chem, 50 (1983) 138.